JOURNAL OF CATALYSIS **111**, 136–145 (1988)

The Nature of the SMSI State of the Pt/TiO$_2$ System

TANG SHENG, XIONG GUOXING, AND WANG HONGLI[1]

Dalian Institute of Chemical Physics, Chinese Academy of Sciences, Dalian, China

Received April 2, 1987; revised November 30, 1987

Sputtered samples of Pt/TiO$_2$ and TiO$_2$/Pt and cosputtered samples of Pt–TiO$_2$ have been prepared and studied by TEM, electron diffraction, AES, Auger profiling, and XPS to determine the nature of the SMSI state induced in these samples after high-temperature (~500°C) treatment in hydrogen. Based mainly on observations that the surface was enriched with, not depleted of, platinum, and that TiO$_x$ species with Ti in the 2+ oxidation state and x close to 1 actually diffused into the platinum, it is proposed that the SMSI state of the Pt/TiO$_2$ system is intimately associated with the formation of an intermediate surface compound of the type Pt$_n$TiO$_x$, where n is probably greater than 1 and x is close to 1. This process of surface compound formation is greatly facilitated in the presence of hydrogen. © 1988 Academic Press, Inc.

1. INTRODUCTION

The anomalous adsorption behavior of hydrogen and CO at room temperature after high-temperature reduction by hydrogen on Pt/TiO$_2$ and similar systems was first reported by Tauster *et al.* (*1*). Although many attempts to elucidate the nature of this so-called "strong metal-support interaction" (SMSI) have been made from different angles with some degree of success, opinions still differ. Experimental results sometimes even contradict each other and the true nature of the SMSI state remains evasive. A charge transfer mechanism was proposed both theoretically (*2*) and experimentally (*3*), but the direction and magnitude of this proposed charge transfer still seem somewhat uncertain. A model based on morphological change was put forward (*4*) which seems to require further refinement. The role of hydrogen in the manifestation of SMSI behavior for the Pt/TiO$_2$ system was stressed (*5*) and more work along this line appears to be desirable. The emergence of a reactive interface between the metal and the support, with the creation of new active sites along the boundary, has been advocated (*6*) and has gained support from recent experimental (*7–11*) as well as theoretical (*12*) work. Lately, a surface migration of TiO$_x$ species and the resultant site-blocking mechanism were advanced (*13–21*) and apparently explained the experimental findings of quite a few model systems.

We would like to point out, however, that all the model systems reported to date appear to have the drawback of studying the metal/support interface from only one side of the interface and presenting a limited interfacial area. This could hardly depict the true picture of a conventionally prepared catalyst system. In addition, such investigations were often made only after UHV treatment of the sample, neglecting the effect of hydrogen. It is the aim of this work to simulate and study the SMSI system of Pt/TiO$_2$ with sputtered and cosputtered samples in which the crystallites of metal and support are in intimate contact. Furthermore, the interface between the metal and the support may be studied from both sides and under identical conditions in the cosputtered samples.

The sputtered systems thus obtained have the distinct advantage of being extensive in interfacial area, easily controllable in composition, homogeneous, and quite suitable for surface measurements. Our ex-

---

[1] To whom correspondence should be addressed.

0021-9517/88 $3.00

perimental data, which were obtained after UHV as well as hydrogen treatment at high temperatures, are consistent with the description that the SMSI state of Pt/TiO_2 system is associated with the formation of an intermediate surface compound of the type Pt_nTiO_x, in which a strong interaction between Pt and Ti is characterized by the presence of a stabilized Ti^{2+} species and the enrichment of Pt on the surface. The value of x in the Pt_nTiO_x surface compound is most likely close to 1, and n is probably greater than 1. Furthermore, this process of forming an intermediate compound on the surface is greatly facilitated in the presence of hydrogen.

2. EXPERIMENTAL

2.1. *Catalyst Preparation*

Three kinds of Pt supported on TiO_2 catalyst samples were prepared by sputtering, namely, the normally supported catalyst, the inversely supported catalyst, and the cosputtered catalyst. The normally supported Pt/TiO_2 sample was prepared by sputtering platinum from a Pt foil (diameter 10 mm, thickness 0.1 mm) as the cathode onto a sputtered film of TiO_2, which was obtained by using a compressed pellet of TiO_2 as the cathode. The TiO_2 powder used was analytically pure and the platinum foil was supplied by BDH Company of England with a purity of greater than 99.9%. The inversely supported sample of TiO_2/Pt was prepared by sputtering the TiO_2 target which is in the form of a compressed pellet (diameter 30 mm, thickness 2 mm) onto a sputtered platinum film. For the cosputtered samples of $Pt–TiO_2$, a composite target composed of a 10-mm platinum thin foil imbedded in a compressed pellet of TiO_2 (30 mm in diameter) was used as the cathode. The working vacuum of the sputtering apparatus was 10^{-6} Torr (133.3 Torr = 1 N m^{-2}). Mica sheets were used as the substrate for most samples. Ti and Ta foils were also used when required. The thickness of the sputtered films was obtained by making Auger depth profiles. Samples prepared in this way are listed in Table 1. The thickness of the films is given in parentheses.

The cosputtered sample of Pt–TiO was designed to be used to study directly the possible migration of TiO species into Pt and was prepared by using a composite target consisting of a Pt foil and a partially oxidized titanium foil. The O/Ti ratio as determined from XPS *O* 1*s*/Ti 2*p* peak areas was found to have the relative values of 2.0 to 1.1 for the samples of $Pt–TiO_2$ and Pt–TiO.

Samples used in the electron microscope study, several nanometers in thickness, were prepared by direct sputtering onto an amorphous carbon film supported by a stainless-steel grid.

2.2. *Catalyst Characterization*

Particle size determinations of the sputtered samples were made on a Hitachi H-600 Analytical Electron Microscope. Interplanar spacings of the metal particles were determined from the electron diffraction rings obtained from a 100-keV electron beam on the same apparatus. The probable error is estimated to be ±0.015 Å.

XPS, AES, and Auger profiling were performed on a PHI 550 ESCA/SAM apparatus. XPS data were taken with Mg or Al *Kα* radiation (1253.6 or 1486.6 eV, respectively) at an acceleration voltage of 10 kV and an electron current of 35 mA. The base pressure of the UHV apparatus was 1.2×10^{-10} Torr. Samples were pretreated in a preparation chamber as required before transfer to the spectrometer chamber. The charging effect of various samples was min-

TABLE 1

Pt/TiO_2 Samples Prepared

Sample	Type	Substrate
Pt(20 nm)/TiO_2(20 nm)	Normally supported	Ta foil
TiO_2(5 nm)/Pt(20 nm)	Inversely supported	Mica sheet
$Pt–TiO_2$ (40 nm)	Cosputtered	Mica sheet

imized by taking reference to the binding energy of C 1*s* for the contaminated carbon (284.6 eV) as the internal standard. The surface composition, expressed as the relative atomic ratios of different components, was calculated from the relative peak areas of XPS spectra by using sensitivity factors supplied by the "PHI Handbook." The deconvolution of XPS spectra into Ti^{4+}, Ti^{3+}, and Ti^{2+} components was carried out by a computer program based on the data given in the work of Sayers and Armstrong (*22*).

The electron beam energy for the Auger measurements was 3 kV and the beam current, 3 μA. The ion sputtering rate was 2–3 nm/min under most conditions. The amount of CO adsorbed was obtained from the relative peak heights of C (272 eV)/Pt (64 eV) as described in the literature (*23*).

Linde research-grade CO containing no less than 99.97% CO was directly used without further purification in characterizing the SMSI state.

3. RESULTS

3.1. Particle Size Variation and CO Adsorption

A transmission electron micrograph of a cosputtered sample of Pt–TiO_2 after hydrogen reduction at 550°C for 2 h is shown in Fig. 1. The particle size distribution for this sample after treatment in hydrogen at different temperatures, as determined by TEM, is shown in Fig. 2. It is seen that the average particle size of the Pt–TiO_2 sample is in the neighborhood of 2.0 nm and the crystallites are evenly distributed on the surface. No appreciable change in particle size was detected for hydrogen treatment

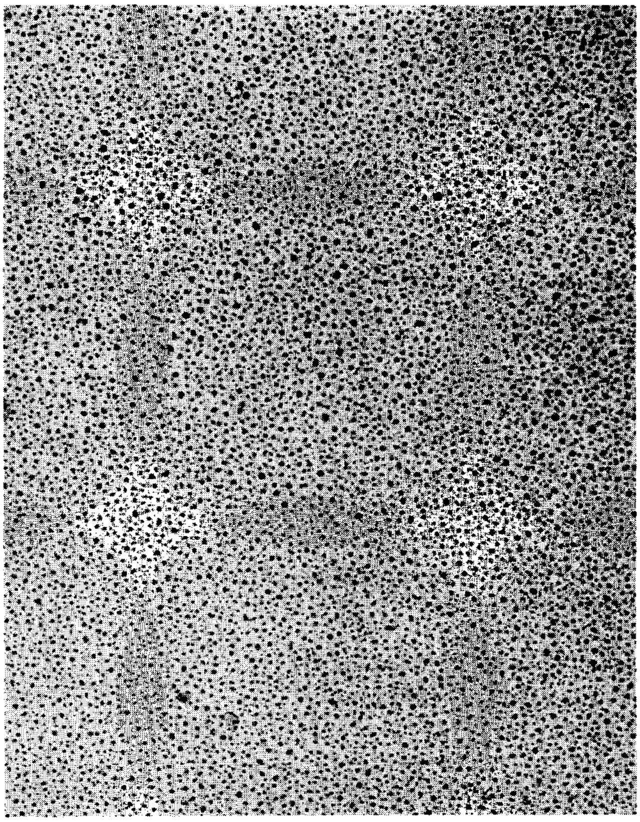

FIG. 1. Transmission electron micrograph of Pt–TiO_2 after H_2 reduction at 550°C for 2 h.

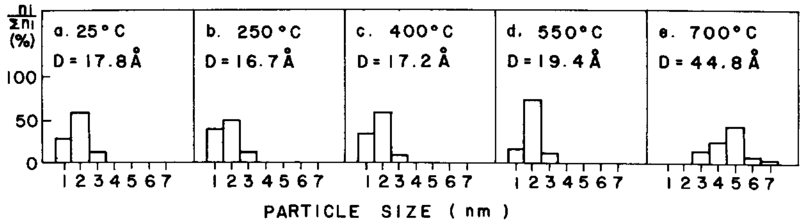

FIG. 2. Particle size distribution of Pt–TiO$_2$ after treatment in H$_2$ at different temperatures for 2 h.

up to 550°C. However, reduction at 700°C significantly increased the average particle size from about 2 nm to greater than 4 nm, indicating that some coalescence of particles has taken place. For the sputtered samples of Pt/TiO$_2$ and TiO$_2$/Pt, there was no problem of particle size variation. The amounts of CO adsorbed on the Pt–TiO$_2$ sample after different treatments in hydrogen are listed in Table 2.

3.2. Change in Interplanar Spacing as a Result of Hydrogen Treatment

The interplanar spacing between (111) planes, *d*(111), of Pt changes after hydrogen reduction at different temperatures and other treatments. The values determined by electron diffraction for platinum foil and Pt–TiO samples are listed in Table 3. Five new electron diffraction rings not present for Pt were found for the Pt–TiO$_2$ sample after hydrogen reduction at 700°C. The *d* spacings of these crystallographic planes, obtained from the 100-keV electron diffraction study for the Pt–TiO$_2$ sample after 700°C hydrogen treatment, are listed in Table 4 and are consistent with the formation of Pt$_3$Ti as the result of hydrogen reduction at 700°C.

3.3. Auger Electron Spectra and Auger Profiles

Auger electron spectra for Pt/TiO$_2$ sample before and after treatment at 700°C in UHV for 1 h are shown in Fig. 3. Neither Ti nor O could be detected in the spectra before treatment. The Auger profiles for the same sample before and after treatment in UHV at 700°C for 1 h are shown in Fig. 4. The sputtering rate was about 3 nm/min. It is seen that while the concentrations of Ti and O in the Pt film are approximately constant, the O/Ti ratio changes radically as the boundary between the Pt film and the TiO$_2$ film is crossed.

The Auger electron spectra and the Auger profiles for the inversely supported sample of TiO$_2$/Pt before and after different treatments are shown in Figs. 5 and 6 respectively. It is seen from Fig. 5 that no Pt could be found in the TiO$_2$ film before

TABLE 2

Amounts of CO Adsorbed on Pt–TiO$_2$ after Treatment in H$_2$ at Different Temperatures

Temperature (°C)	Amount of CO adsorbed, C(272 eV)/Pt(64 eV)
Before treatment	0.333
250	0.234
400	0.109
550	0.085

TABLE 3

Change in Interplanar Spacing *d*(111) for Pt Foil and Pt–TiO after Different Treatments

Treatment	*d*(111) (Å), Pt foil	Treatment	*d*(111) (Å), Pt in Pt–TiO
Standard value (*24*)	2.265	Untreated	2.25
300°C, Ar	2.26	300°C, Ar	2.37
300°C, H$_2$	2.29	300°C, H$_2$	2.36
500°C, H$_2$	2.33	500°C, H$_2$	2.35
700°C, Ar	2.22	700°C, Ar	2.36
700°C, H$_2$	2.31	700°C, H$_2$	2.29
500°C, O$_2$	2.26	500°C, O$_2$	2.34

TABLE 4

Interplanar Spacings for Certain Crystallographic Planes of Pt_3Ti and Pt–TiO_2 after 700°C H_2 Reduction

Pt_3Ti (*25*)		Pt–TiO_2
(*h k l*)	*d* (Å)	*d* (Å)
1 0 0	3.87	3.91
1 1 0	2.743	2.77
2 1 0	1.742	1.75
2 1 1	1.591	1.60
3 2 1	1.043	1.05
3 0 0, 2 2 1	1.3	—
3 1 0	1.235	—

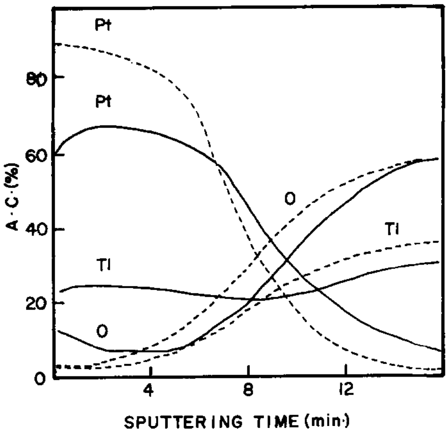

FIG. 4. Auger profiles for Pt/TiO_2: (---) untreated sample, (—) sample treated in UHV at 700°C for 1 h.

treatment or after treatment at 500°C in UHV for 1 h. But, after treatment in hydrogen at 500°C for 1 h, a strong Pt signal was observed and the intensity of the Ti and O signals was greatly diminished. The Auger profiles shown in Fig. 6 further indicate that after hydrogen treatment at 500°C for 1 h the concentrations of Ti and O remain approximately constant in the Pt film and the O/Ti ratio changes very markedly.

3.4. XPS Spectra

For the study of surface composition and interdiffusion of components of TiO_2/Pt and Pt/TiO_2 samples the Ti 2*p* spectra for these samples are shown in Fig. 7 and those for the cosputtered Pt–TiO_2 samples are shown in Fig. 8. The relative atomic ratios of different species of Ti and the Pt/Ti and O/Ti ratios on the surface of the Pt–TiO_2 sample calculated from the XPS peak areas are shown in Table 5.

It is seen that for the normally supported Pt/TiO_2 sample, no species of Ti was present before treatment. But after UHV treatment at 700°C for 1 h, in addition to Ti^{4+}, titanium ions with lower oxidation state, Ti^{3+} and Ti^{2+}, were also present on the surface. For the inversely supported TiO_2/Pt

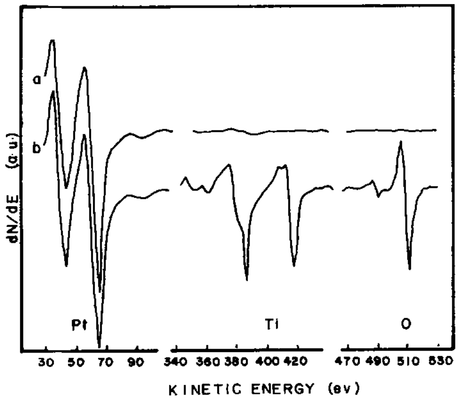

FIG. 3. Auger electron spectra for Pt/TiO_2: (a) untreated sample, (b) sample treated in UHV at 700°C for 1 h.

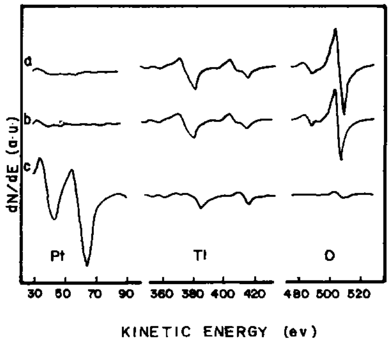

FIG. 5. Auger electron spectra for TiO_2/Pt: (a) untreated sample, (b) sample treated in UHV at 500°C for 1 h, (c) sample treated in hydrogen at 500°C for 1 h.

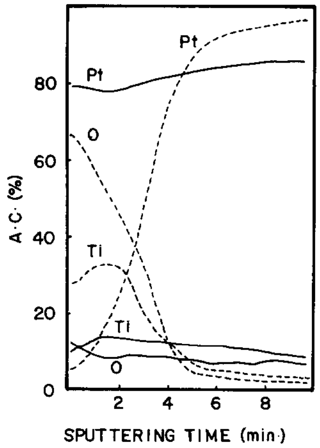

FIG. 6. Auger profiles for TiO$_2$/Pt: (---) untreated sample, (—) sample treated in H$_2$ at 500°C for 1 h. Sputtering rate: about 3 nm/min.

sample only Ti^{4+} with a binding energy of 458.6 ± 0.2 eV was present before treatment. But after treatment in hydrogen at 500°C for 1 h, the Ti $2p_{3/2}$ peak at 455.0 ± 0.2 eV binding energy was found to dominate and may be assigned to Ti^{2+} species. UHV treatment at 500°C for 1 h, on the other hand, did not produce any Ti^{2+}. For the cosputtered Pt/TiO$_2$ sample, hydrogen reduction at 550°C for 1 h produced 12% Ti^{2+} and 26% Ti^{3+}, with a binding energy of 456.5 ± 0.2 eV on the surface. It should be pointed out that, for this sample, the Pt/Ti ratio increased after hydrogen treatment at 550°C. AES measurements gave qualitatively the same result.

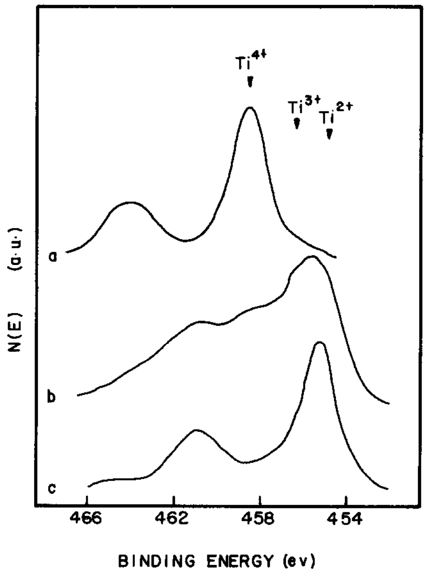

FIG. 7. Ti $2p$ spectra of TiO$_2$/Pt and Pt/TiO$_2$ samples: (a) TiO$_2$/Pt treated in UHV at 500°C for 1 h, (b) Pt/TiO$_2$/Ta treated in UHV at 700°C for 1 h, (c) TiO$_2$/Pt treated in H$_2$ at 500°C for 1 h.

4. DISCUSSION

4.1. *Pt Enrichment of the Surface*

It is interesting to compare the different behavior of Pt/TiO$_2$, TiO$_2$/Pt, and Pt–TiO$_2$ samples before and after either UHV or hydrogen treatment at high temperatures (~500°C) as revealed by the XPS study (Table 5). For Pt/TiO$_2$, the Pt/Ti ratio decreased as the result of high-temperature UHV treatment; a more severe drop in the Pt/Ti ratio is expected after high-temperature hydrogen reduction, as found by many workers in this field, and is ascribed to TiO$_x$ migration (discussed later). AES measurements were also made on all catalyst systems to determine the surface composition before and after treatments. The results ob-

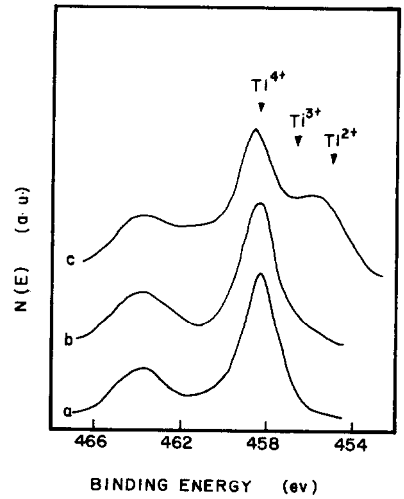

FIG. 8. Ti $2p$ spectra of the Pt–TiO$_2$ sample: (a) untreated, (b) treated in UHV at 550°C for 1 h, (c) treated in H$_2$ at 550°C for 1 h.

TABLE 5

Surface Composition of Pt/TiO_2, TiO_2/Pt, and $Pt\text{-}TiO_2$ Samples

Sample	Pretreatment	Relative content of different Ti species			Relative atomic ratio on surface	
		Ti^{4+}	Ti^{3+}	Ti^{2+}	Pt/Ti	O/Ti
Pt/TiO_2	Untreated	0	0	0		
	UHV, 700°C, 1 h	0.19	0.39	0.42	3.08	1.1
TiO_2/Pt	Untreated	1.0	0	0	0	2.03
	UHV, 500°C, 1 h	0.97	0.03	0	0.07	2.06
	H_2, 500°C, 1 h	0.09	0.12	0.79	15.6	
$Pt\text{-}TiO_2$	Untreated	1.0	0	0	0.33	2.06
	UHV, 550°C, 1 h	0.92	0.08	0	0.36	1.87
	H_2, 550°C, 1 h	0.62	0.26	0.12	0.45	0.75

tained were in general agreement, at least qualitatively, with the XPS data given in Table 5.

In the case of the cosputtered $Pt\text{-}TiO_2$ sample, however, the Pt/Ti ratio obtained from the XPS data showed successive increases when treated at 550°C first in UHV for 1 h and then in hydrogen for another hour. Enrichment, not depletion, of surface Pt was observed. On a conventionally prepared Pt/TiO_2 system catalyst previously reported (*5*), a similar Pt enrichment on the surface of the catalyst was noted upon hydrogen treatment at high temperatures. This Pt enrichment cannot be explained by a simple TiO_x migration mechanism. It is more likely due to the migration or spreading (*4*) of Pt to the contiguous TiO_2 particles and the formation of an intermediate surface compound with the migrating TiO_x species formed upon partial reduction of TiO_2. The reason this phenomenon has not been observed in other model systems is probably that the interface between Pt and TiO_2 was investigated only from one side in those systems and that attention was consequently directed to the migration of TiO_x alone.

For the TiO_2/Pt sample, the Pt/Ti ratio increased as a result of high-temperature UHV or hydrogen treatment. This cannot be explained by the simple TiO_x migration mechanism either. The migration of Pt was probably also involved.

4.2. Titanium Species Present on the Surface

Much effort has been expended in identifying the titanium species that is present on the surface of the Pt/TiO_2 system after high-temperature hydrogen treatment. But, in early studies, it was difficult to get anything other than a shoulder in the Ti 2*p* spectrum with a binding energy lower than that of Ti^{4+} which may be assigned to Ti^{3+} (*26*). Only recently, Greenlief *et al.* (*27*) were able to characterize by XPS a sample of TiO_2/Pt in which Ti^{3+} was present on the surface of a thin TiO_2 film deposited on a Pt foil after 650 K annealing in oxygen for 30 min.

In Figs. 7 and 8, it is clearly seen that Ti ions of lower oxidation states are present on the surface of Pt/TiO_2 and TiO_2/Pt samples after high-temperature UHV or hydrogen treatment. Ti^{2+} was found to be the major component and Ti^{3+} was also present. For the sample of TiO_2/Pt, which is comparable with the one used by Greenlief *et al.*, except that the TiO_2 film was thicker in our case, only Ti^{3+} was present after treatment in UHV at 500°C for 1 h. This is in qualitative agreement with their result as shown in Table 4. But Ti^{2+} was predominant after hydrogen treatment at the same temperature. Furthermore, the relative atomic ratio O/Ti of the species that was found on the surface of the sample of Pt/TiO$_2$ was much less than 2 and close to 1.

We have also found that the Ti^{2+} species produced on the surface of all the samples examined was stable under ambient conditions. The peak position of this Ti species on the XPS spectrum did not change appreciably after exposure in air. We are inclined to consider, therefore, that the Ti^{2+} species produced on the surface of the Pt/TiO$_2$ system after high-temperature treatment in hydrogen around 500°C is not a simple reduction product of Ti^{4+} but is a species stabilized by the interaction of Pt and Ti.

4.3. Surface Migration of TiO$_x$

The Auger profiles for the samples of Pt/TiO$_2$ and TiO$_2$/Pt shown in Figs. 3 and 4 clearly demonstrate the migration of TiO$_x$ ($x \ll 2$) from the TiO$_2$ film into the Pt film. Furthermore, the relative concentrations of Ti and O species, as seen from the profiles, remain approximately constant throughout the thickness of the Pt film, suggesting the formation of a relatively stable surface compound comprising Pt and TiO$_x$. The migration of TiO$_x$ ($x \sim 1$) into the Pt was also seen from the XPS data for the normally supported Pt/TiO$_2$ sample given in Table 5. The simultaneous presence of Ti^{3+} and Ti^{4+} together with Ti^{2+} could mean the recombination of TiO$_x$ ($x \sim 1$) species after penetration through Pt in this case.

The diffusion of a TiO$_x$ species into bulk Pt on a TiO$_2$/Pt sample at temperatures greater than 700 K has been observed by Ko and Gorte (*19, 20*) by AES measurements. But it was stated that the oxidation state of the migrating species of Ti cannot be determined by Auger electron spectroscopy. In the last section, we reported that a stabilized Ti^{2+} was present on all samples examined after high-temperature hydrogen reduction. That the TiO$_x$ species in which x is close to 1 has diffused into the Pt film may also be seen from the change in interplanar spacings of Pt in the Pt–TiO sample after hydrogen reduction at high temperatures.

The changes in $d(111)$ spacings for Pt foil and the Pt in the Pt–TiO sample were followed after different treatments and are given in Table 3. It can be seen that for Pt foil, $d(111)$ increased with the temperature of hydrogen treatment, but upon flushing with Ar or oxygen, it returned to its initial value, indicating that the penetrated hydrogen that caused the lattice expansion of Pt was removed by such treatment. On the other hand, when the Pt–TiO sample was treated in the same manner, the $d(111)$ values did not return to their original values. This suggests that the species that caused the lattice expansion in this case was not hydrogen as might have been suspected. More likely it was the migrating species TiO. It could not be flushed out by Ar and was regenerated when the Pt–TiO sample reduced at 700°C in hydrogen with the formation of Pt$_3$Ti was exposed to oxygen. This is probably associated with the basic mechanism involved in the reversibility of the SMSI state after reduction and reoxidation.

This migration of TiO$_x$ species ($x \sim 1$) into the Pt film is probably similar in nature to the case found by Bardi and Ross (*28*) for Pt$_3$Ti. In their case the Ti/Pt ratio decreased when the TiO$_{1.2}$ overlayer on Pt$_3$Ti was reduced in hydrogen above 500°C with a constant O/Ti ratio. This may be interpreted as the migration of TiO$_x$ species ($x \sim 1$) into Pt$_3$Ti in addition to, or even instead of, the dissolution of Ti into the bulk Pt$_3$Ti as implicated by Greenlief *et al.* (*27*). The migration of TiO$_x$ species for the Pt/TiO$_2$ system has also been extensively discussed by Spencer (*29*) and experimentally studied by TEM by Vanselow and Mundschaw (*21*) recently.

A very interesting paper was published quite recently (*10*) in which it was stated that the TiO_x species is not simply a site-blocking agent but can also create new chemisorption sites for hydrogen, CO, and NO on various TiO_2-supported transition metal SMSI catalysts. The newly created chemisorption sites resulting from interaction between the transition metal and the TiO_2 support could well be the origin for the enhancement of catalytic activity for certain reactions, such as methanation from CO and hydrogen. Our findings are in accord with this point of view. These "TiO_x-associated dissociation sites," in our opinion, may well be of the type Pt_nTiO_x discussed in this paper.

4.4. *SMSI State of Pt/TiO_2 Systems*

The samples used in this work in the form of sputtered films all exhibit the usual characteristic feature of a SMSI state when treated in hydrogen at high temperatures, namely, the amount of CO adsorbed at room temperature was markedly decreased as a result of this treatment. The particle size, however, did not change appreciably and the Pt/Ti ratio increased not decreased after high-temperature reduction in hydrogen. These observations cannot be interpreted in terms of an encapsulation mechanism nor can they be reconciled with the picture of a simple TiO_x migration with the result of physical site blocking. The platinum of the Pt/TiO_2 system, after high-temperature treatment in hydrogen, is in a special state, the SMSI state.

Any description of this SMSI state of the Pt/TiO_2 system should contain the following features: (1) surface enrichment not depletion of Pt, implying surface migration or spreading of Pt onto the contiguous particles of TiO_2; (2) generation of Ti^{2+} and its stabilization, implying some kind of compound formation which could constitute the driving force for interdiffusion of both Pt and TiO_x; (3) migration of TiO_x ($x \sim 1$) into the platinum and the simultaneous presence of Ti^{4+}, Ti^{3+}, and Ti^{2+}, implying the possible recombination of TiO_x species ($x \sim 1$) on one hand and the incomplete reduction of TiO_2 on the other; (4) transformation of Pt into the intermetallic compound of Pt_3Ti after 700°C hydrogen treatment, implying that this SMSI state of Pt/TiO_2 may be intermediate in nature. In the context of the requirements listed above, it seems reasonable to propose that the SMSI state of the Pt/TiO_2 system is intimately associated with the presence of an intermediate surface compound of the type Pt_nTiO_x in which x is close to 1 and n is probably greater than 1 under the experimental conditions of hydrogen reduction at about 500°C. The chemical properties of this intermediate surface compound with the additional effect of back-spilled hydrogen (*30*) could conceivably be different from those of Pt. The preponderance of Ti^{4+} for the cosputtered Pt–TiO_2 sample after high-temperature hydrogen treatment despite the generation of Ti^{2+} seems to indicate that in addition to the possible recombination of TiO_x ($x \sim 1$) species, this intermediate surface compound Pt_nTiO_x is present only on that part of the Pt particles accessible to the TiO_x migration and on that part of the TiO_2 particles contiguous to the particles of platinum.

This SMSI state is not, however, unique to the Pt/TiO_2 system. We have found that Pd and Ir behave similarly to Pt and these elements appear to constitute one class of the Group VIII transition metals with regard to the SMSI state when supported on TiO_2 and treated in hydrogen at temperatures around 500°C. Other members of the Group VIII transition metals including Rh and Ru, on the other hand, constitute another class of SMSI state under the same conditions which, in contrast with the Pt class, is characterized by the depletion of metal on the surface upon high-temperature reduction in hydrogen and the absence of Ti^{2+} in the XPS spectra. The details of these findings will be reported elsewhere.

5. CONCLUSIONS

It has been shown in this paper that sputtered samples of Pt/TiO_2 and TiO_2/Pt and a cosputtered sample of Pt–TiO$_2$ may be used advantageously as model catalysts for study of the SMSI state of Pt/TiO$_2$ systems. It is demonstrated that as a result of high-temperature (~500°C) reduction in hydrogen, Ti^{2+}, in addition to Ti^{3+}, is generated and stabilized, and subsequently diffuses into Pt in the form of TiO$_x$ where x is close to 1. Concomitantly, contrary to what is expected from a simple TiO$_x$ migration mechanism, the Pt/Ti ratio increases instead of decreases. This implies that Pt diffuses onto the surface of contiguous TiO$_2$ particles; i.e., interdiffusion of the components in the Pt/TiO$_2$ system takes place. An intermetallic surface compound of Pt$_3$Ti is formed upon hydrogen treatment at a still higher temperature of 700°C. These findings are rationalized by the proposal that an intermediate surface compound of the type Pt$_n$TiO$_x$, where n is probably greater than 1 and x is close to 1, is intimately associated with the SMSI state of the Pt/TiO$_2$ system. The formation of this intermediate surface compound is greatly facilitated in the presence of hydrogen.

ACKNOWLEDGMENTS

This work was supported in part by the Science Fund of the Chinese Academy of Sciences. The authors are also grateful to Mr. Cai Hailin for his valuable assistance in TEM experiments.

REFERENCES

1. Tauster, S. J., Fung, S. C., and Garten, R. L., *J. Amer. Chem. Soc.* **100,** 170 (1978).
2. Horsley, J. A., *J. Amer. Chem. Soc.* **101,** 2870 (1978).
3. Kao, C. C., Tsai, S. C., Bahl, M. K., and Chung, Y-W., *Surf. Sci.* **95,** 1 (1980).
4. Baker, R. T. K., Prestridge, E. B., and Garten, R. L., *J. Catal.* **59,** 293 (1978).
5. Wang, H-L., Tang, S., Xie, M-S., Xiong, G-X., and Guo, X-X., *in* "Metal-Support and Metal-Additive Effects in Catalysis" (B. Imelik *et al.,* Eds.), Elsevier, Amsterdam, 1982.
6. Burch, R., and Flambard, A. R., *J. Catal.* **78,** 389 (1982).
7. Simoens, A. J., Baker, R. T. K., Dwyer, D. J., Lund, C. R. F., and Madon, R. J., *J. Catal.* **86,** 359 (1984).
8. Vannice, M. A., and Sudhaker, C., *J. Phys. Chem.* **88,** 2429 (1984).
9. Levin, M., Salmeron, M., Bell, A. T., and Somorjai, G. A., *Surf. Sci.* **169,** 123 (1986).
10. Belton, D. N., Sun, Y-M., and White, J. M., *J. Catal.* **102,** 338 (1986).
11. Herrmann, J. M., Gravelle-Rumeau-Maillot, M., and Gravelle, P. C., *J. Catal.* **104,** 136 (1987).
12. Li, Y., Chen, R., Xiong, G-X., and Wang, H-L., *J. Mol. Catal.* **42,** 337 (1987).
13. Santos, J., Phillips, J., and Dumesic, J. A., *J. Catal.* **81,** 147 (1983).
14. Cairns, J. A., Baglin, J. E. E., Clark, G. J., and Ziegler, J. F., *J. Catal.* **83,** 301 (1983).
15. Sadeghi, H. R., and Henrich, V. E., *J. Catal.* **87,** 279 (1984).
16. Belton, D. N., Sun, Y-M., and White, J. M., *J. Phys. Chem.* **88,** 5172 (1984).
17. Resasco, D. E., and Haller, G. L., *J. Catal.* **82,** 279 (1983).
18. Dwyer, D. J., Cameron, S. D., and Gland, J., *Surf. Sci.* **159,** 430 (1985).
19. Ko, C. S., and Gorte, R. J., *J. Catal.* **90,** 59 (1984).
20. Ko, C. S., and Gorte, R. J., *Surf. Sci.* **155,** 296 (1985).
21. Vaselow, R., and Mundschau, M., *J. Catal.* **103,** 426 (1987).
22. Sayers, C. N., and Armstrong, N. R., *Surf. Sci.* **77,** 301 (1978).
23. Kao, C. C., Tsai, S-C., and Chung, Y-W., *J. Catal.* **73,** 136 (1982).
24. "Powder Diffraction File," Inorganic Vol. No. PDIS-5iRB, 04-802, Swarthmore, JCPDS, 1980.
25. "Powder Diffraction File," Inorganic Vol. No. PDIS-18iRB, 17-64, Swarthmore, JCPDS, 1980.
26. Tauster, S. J., and Fung, S. C., *J. Catal.* **55,** 29 (1978).
27. Greenlief, C. M., White, J. M., Ko, C. S., and Gorte, R. J., *J. Phys. Chem.* **89,** 5025 (1985).
28. Bardi, U., and Ross, P. N., *J. Vac. Sci. Technol. A* **2**(4), 1461 (1984).
29. Spencer, M. S., *J. Catal.* **93,** 216 (1985).
30. Hu, J-H., Hong, Z-P., Song, Y-Z., and Wang, H-L., *Stud. Surf. Sci. Catal.* **17,** 53 (1983).